The rab Exchange Factor Sec2p Reversibly Associates with the Exocyst[D]

Martina Medkova, Y. Ellen France, Jeff Coleman, and Peter Novick

Department of Cell Biology, Yale University School of Medicine, New Haven, CT 06510

Activation of the rab GTPase, Sec4p, by its exchange factor, Sec2p, is needed for polarized transport of secretory vesicles to exocytic sites and for exocytosis. A small region in the C-terminal half of Sec2p regulates its localization. Loss of this region results in temperature-sensitive growth and the depolarized accumulation of secretory vesicles. Here, we show that Sec2p associates with the exocyst, an octameric effector of Sec4p involved in tethering secretory vesicles to the plasma membrane. Specifically, the exocyst subunit Sec15p directly interacts with Sec2p. This interaction normally occurs on secretory vesicles and serves to couple nucleotide exchange on Sec4p to the recruitment of the Sec4p effector. The mislocalization of Sec2p mutants correlates with dramatically enhanced binding to the exocyst complex. We propose that Sec2p is normally released from the exocyst after vesicle tethering so that it can recycle onto a new round of vesicles. The mislocalization of Sec2p mutants results from a failure to be released from Sec15p, blocking this recycling pathway.

INTRODUCTION

In the final stage of the yeast exocytic pathway, secretory vesicles are actively transported to sites of polarized growth, including the tips of small buds early in the cell cycle and mother-daughter necks late in the cycle. Polarized vesicle delivery relies on the actin cytoskeleton and Myo2p, a class V myosin motor (Novick and Botstein, 1985; Govindan *et al.*, 1995; Pruyne *et al.*, 1998; Karpova *et al.*, 2000). Although most mutants defective in Golgi-to-plasma membrane transport are blocked downstream of vesicle delivery, temperature-sensitive mutations in *sec2* cause an accumulation of vesicles randomly distributed throughout the cytoplasm, similar to that seen in *act1–1* and *myo2–66* cells (Walch-Solimena *et al.*, 1997). This implies that activation of Sec4p by its exchange factor, Sec2p, is necessary for the vectorial delivery or retention of vesicles at sites of secretion. Both Sec4p and Sec2p are found in association with secretory vesicles as they are delivered to exocytic sites (Walch-Solimena *et al.*, 1997). On arrival, vesicles are tethered to the plasma membrane through an association with the exocyst complex. The exocyst functions as a Sec4p effector and consists of eight subunits: Sec3p, Sec5p, Sec6p, Sec8p, Sec10p, Sec15p, Exo70p, and Exo84p (TerBush *et al.*, 1996). Sec3p associates with the plasma membrane independent of membrane traffic and acts as a spatial landmark for secretory vesicles (Finger *et al.*, 1998), whereas Sec15p associates with secretory vesicles and directly contacts Sec4p (Guo *et al.*, 1999). The other exocyst subunits are, like Sec15p, transported on vesicles (Boyd *et al.*, 2004). Exocyst assembly occurs as vesicles arrive at sites marked by Sec3p.

Association of Sec2p with secretory vesicles is important for its function. A stretch of 58 amino acids (aa.451-508) within the C-terminal half of the molecule is necessary, but not sufficient for membrane association (Elkind *et al.*, 2000). Loss of this region in truncated alleles (*sec2-59*, *sec2-41*) or a point mutation within this domain (*sec2-78*) has no effect on the exchange activity measured in vitro, yet severely impairs Sec2p localization, yielding a temperature-sensitive growth and secretion phenotype. A mammalian homologue of Sec2p, Rabin8, is required for polarized delivery of Rab8-specific vesicles to the cell surface and the carboxy terminus of Rabin8 is essential for this process (Hattula *et al.*, 2002). Two rab GTPases, in addition to Sec4p, have been shown to directly interact with Sec2p. These are the redundant proteins Ypt31p and Ypt32p that control exit from the Golgi (Ortiz *et al.*, 2002). Together, these components constitute a signaling cascade, in which Ypt31/32p in the GTP-bound state recruits Sec2p to the secretory vesicle membrane, leading to the activation of the downstream GTPase Sec4p. Overexpression of Ypt32p suppresses the growth defect of *sec2-78* and restores the localization of Sec2-78-GFPp. Interestingly, overexpression of Ypt32p also restores the localization of Sec2-59-GFPp, a truncated allele missing the entire carboxy-terminal half of the protein. This is consistent with the finding that the binding site for Ypt32p is located in the amino terminal half of Sec2p, just downstream of the exchange domain. Nonetheless, it raises two related questions: Why are Sec2-59p and Sec2-78p mislocalized, because they contain the Ypt32p binding site? and What is the function of the region between amino acids 451-508, because it is not needed for Ypt32p binding? There must be an additional factor or mechanism regulating Sec2p membrane attachment.

An emerging theme in the small GTPase field is that exchange factors can associate with specific effectors of the GTPases they activate. A well characterized example is the Rabex5/Rabaptin5 complex that functions early in the endocytic pathway (Horiuchi *et al.*, 1997). Rabex5 is a guanine

nucleotide exchange factor (GEF), and Rabaptin5 is an effector for the small GTPase Rab5. Rabex5 is involved in Rab5-dependent recruitment of Rabaptin5 to early endosomes, Rabaptin5 in turn increases the exchange activity of Rabex5 (Lippe *et al.*, 2001). Another example is the class C/HOPS complex that functions in homotypic vacuole fusion and contains both an exchange factor and effector of the rab GTPase, Ypt7p (Seals *et al.*, 2000; Wurmser *et al.*, 2000). It is thought that by physically linking an effector to an exchange protein, a localized microdomain of activated rab protein can be established and maintained.

In the present study, we show that Sec2p associates with the exocyst through a direct interaction with the Sec15p subunit and that the mislocalization of Sec2p mutants correlates with dramatically enhanced binding to Sec15p. We propose a cycle in which Sec2p is normally released from the exocyst after vesicle tethering. Sec2p mutants defective in the region of 450-508 aa display increased binding to Sec15p and are therefore unable to recycle onto a new round of secretory vesicles, resulting in Sec2p mislocalization and impaired secretion.

MATERIALS AND METHODS

Plasmid Construction and Strains

The construction of various *GST-Sec2* truncations in the vector pNB529 (integrating yeast vector with *GAL1* promoter and *ADH1* terminator) was described previously (Ortiz *et al.*, 2002). The DNA region coding for GST-Sec2(aa.1-258) was amplified from pNB1152 (*SEC2* in pGex4T-1); the DNA regions coding for GST-Sec2(aa.161-258) and GST-Sec2(aa.161-374) were amplified from pNB1158 by using the same primers as described previously (Ortiz *et al.*, 2002). The products were digested with PstI and HindIII enzymes and ligated into the vector pNB529. The resulting plasmids linearized with ClaI were introduced into the protease-deficient *pep4::HIS3* yeast strain NY603. For list of strains, see Table 1. To induce protein expression, cells were grown in YP medium containing 2% galactose.

Glutathione S-Transferase (GST) Pull Downs from Yeast

We resuspended 50–75 optical density (OD) units of yeast overexpressing GST-Sec2p or GST-Sec2 truncations in lysis buffer containing $1\times$ PBS, 0.5% Triton X (TX)-100, 5 mM dithiothreitol [DTT] and protease inhibitors. Cells were disrupted in a bead beater by using 0.5 mm zirconia/silica beads (beads and instrument from Biospec Products, Bartlesville, OK). Lysates were then cleared by centrifugation at $16,000 \times g$ for 10 min at 4°C. Triton X-100 was adjusted to 1%, and supernatants were then incubated with 400 μl of a 50% (vol/vol) slurry of glutathione-Sepharose 4B beads (Amersham Biosciences, Uppsala, Sweden) for 60 min while rotating the samples at 4°C. After the incubation, the beads were spun at $5000 \times g$ and washed four times with 1 ml of ice-cold phosphate-buffered saline (PBS).

Purification of the Exocyst Complex

The intact exocyst complex was isolated from the yeast strain NY2520 by using C-terminally tandem affinity purification (TAP)-tagged subunit Exo70p. Yeast, grown to OD_{600} 1.5, were lysed in a buffer of 20 mM PIPES, pH 6.8, 150 mM NaCl, 1 mM EDTA, 0.2 mM phenylmethylsulfonyl fluoride [PMSF], 10 μM antipain, 20 μM aprotinin, 20 μM chymostatin, 20 μM leupeptin, 20 μM pepstatin A, and 10 mM β-mercaptoethanol by using a Bead Beater (Biospec Products). The 30-ml chamber was half-filled with 0.5-mm glass beads (Biospec Products) and run 4×1 min. NP-40 (IGEPAL CA-630; Sigma-Aldrich, St. Louis, MO) was added [0.5% (vol/vol)], and the lysates were incubated at 4°C for 15 min and then centrifuged at $30,000 \times g$ for 15 min. The method for protein isolation in Puig *et al.* (2001) was followed except 20 mM PIPES, pH 6.8, was substituted for Tris-HCl in all buffers, the tobacco etch virus proteinase incubation was allowed to proceed overnight at 4°C, and the concentration of EGTA in the elution buffer was increased to 10 mM (Puig *et al.*, 2001).

Expression and Purification of GST-Sec2 and Hexahistidine-tagged (His_6) Exocyst Subunits in *Escherichia coli*

GST-Sec2p in pGEX4T-1 (pNB1152) was transformed into *E. coli* BL21 cells. Cells were grown at 37°C to an OD_{600} of 1 and induced using 0.4 mM isopropyl-β-D-thiogalactopyranoside (IPTG) for 3 h at 37°C. The resulting fusion protein was purified according to the manufacturer's protocol. Briefly, the bacterial pellet was resuspended in $1\times$ PBS buffer containing 5 mM DTT and protease inhibitors. Cells were disrupted by sonication, Triton X-100 was

added to the suspension to a final concentration of 1% followed by 30-min incubation on ice. The suspension was then cleared by centrifugation. After a 60-min incubation with GST-Sepharose beads, the beads were extensively washed with $1\times$ PBS buffer and used for in vitro binding experiments.

Exocyst genes were PCR amplified and cloned using the pET-46 Ek/LIC cloning kit (Novagen, Madison, WI). Constructs were transformed into Rosetta 2 cells (Novagen) and grown in Terrific broth at 25°C to an OD_{600} of 1. Cultures were chilled on ice for 30 min and then induced using 0.1 mM IPTG for 16 h at 15°C. The cells were pelleted, resuspended in a buffer of $1\times$ PBS, 160 mM NaCl, 15 mM imidazole, and 1 mM PMSF, and lysed using a Branson Sonifier 450 sonicator (4 times for 1 min). Triton X-100 was added [1% (vol/vol)], and the lysates were incubated at 4°C for 30 min and then centrifuged at $30,000 \times g$ for 15 min. Fusion proteins were isolated using Ni-NTA agarose (QIAGEN, Valencia, CA) for 1.5 h at 4°C. The resin was washed with $1\times$ PBS, 160 mM NaCl, 1% Triton X-100, and 25 mM imidazole, and fusion proteins were eluted with the same buffer, except the imidazole concentration was raised to 400 mM. (His_6)-Ypt32p was purified from *E. coli* as described previously (Du and Novick, 2001).

In Vitro Binding Assay

GST-Sec2 fusion protein immobilized on glutathione-Sepharose beads was incubated with (His_6)-Ypt32p in $1\times$ PBS buffer containing 1 mg/ml bovine serum albumin (BSA), 1 mM DTT, and 1 mM $MgCl_2$. The total volume of incubation mixtures was 400 μl. After incubating for 60 min at room temperature, the resin was washed with the incubation buffer without BSA, and bound products were separated by sodium dodecyl sulfate-polyacrylamide gel electrophoresis (SDS-PAGE). To preload Ypt32p with guanosine 5′-*O*-(3-thio)triphosphate (GTPγS), 5 μM protein was incubated with 1 mM nucleotide in $1\times$ PBS buffer containing 1 mg/ml BSA, 1 mM EDTA, 1 mM $MgCl_2$, and 1 mM DTT for 1 h at 30°C.

The binding of exocyst subunits to GST-Sec2p was conducted in a similar manner except that the binding reactions were performed in a buffer containing $1\times$ PBS, 1 mg/ml BSA, and 0.25% Triton X-100.

Limited Proteolysis of Sec2p

Limited tryptic digestion of GST-Sec2p and GST-Sec2-78(C483Y) proteins was carried out at room temperature in a buffer containing 50 mM Tris, pH 8.0, 100 mM NaCl, and 1 mM DTT. GST-Sec2p fusion proteins were purified from yeast as described previously. One hundred microliters of a 50% (vol/vol) slurry of glutathione-Sepharose 4B (Amersham Biosciences) beads with GST-Sec2 fusion proteins attached (estimated GST-Sec2p concentration is 50 μg/ml) was incubated with *N*-tosyl-L-phenylalanine chloromethyl ketone-treated trypsin (Sigma-Aldrich). The trypsin/GST-Sec2p (wt/wt) ratio was 1:25. Twenty microliters aliquots was withdrawn at indicated time intervals, mixed with SDS sample buffer and immediately boiled for 5 min. Proteolytic fragments were separated by SDS-PAGE and detected by Western blot analysis using αGST and αSec2p.

Cell Fractionation and Immunoprecipitation

Cells (200 OD_{600} units) were grown overnight in YPD at 25°C. The procedures for spheroplasting, lysis, and differential centrifugation of the resulting yeast lysates were described previously (Walch-Solimena *et al.*, 1997). Lysates were generated in lysis buffer (20 mM triethanolamine [TEA]-acetate, pH 7.2, 0.8 M sorbitol, 1 mM EDTA, and protease inhibitors). Supernatant S100 and pellet P100 used for immunoprecipitation experiments were prepared from fraction S10 ($10,000 \times g$ supernatant) by centrifugation at $100,000 \times g$ for 20 min at 4°C. The P100 pellet was solubilized in lysis buffer containing 1% Triton X-100 and cleared by spinning briefly at $10,000 \times g$. S100 and solubilized P100 were precleared by incubation with 50 μl of protein G-Sepharose (50% slurry) for 30-min rocking at 4°C. Sec2-GFPp was immunoprecipitated with α-green fluorescent protein (αGFP) rabbit polyclonal antibody overnight at 4°C. Protein G-Sepharose (50 μl of a 50% slurry/1 ml of lysate) was added and incubated for 60 min at 4°C. Beads were then washed four times with 1 ml of PBS buffer. Proteins were resolved by SDS-PAGE and detected by Western blot analysis.

Glycerol Velocity Gradient Fractionation

Yeast (30 OD_{600} units) were disrupted using a bead beater in a buffer containing 20 mM HEPES, pH 7.0, 120 mM NaCl, 1 mM EDTA, 1 mM DTT, 1% TX-100, and protease inhibitors. After spinning at $20,000 \times g$ in a microcentrifuge, the supernatants (300 μl) were loaded onto 5-ml 10–35% glycerol gradients and centrifuged at 50,000 rpm for 5 h in an SW50.1 rotor (Beckman Coulter, Fullerton, CA) at 4°C. Then, 340-μl fractions were collected from the top of the gradient and analyzed by Western blotting. Portions (200 μl) of fractions 4–9 were subjected to immunoprecipitation with anti-GFP antibody. Sec15-13xmycp in the immunoprecipitates was detected by anti-myc. Densitometric measurements of the Western blot were performed using NIH Image 1.62 software.

Table 1. Strain list

Strain	Genotype
NY603	*MATα leu2-3,112 ura3-52 pep4::URA3 GAL+*
NY1060	*MAT**a**/α ura3-52/ura3-52; leu2-3,112/leu2-3,112 GAL+*
NY1562	*MAT**a**/α ura3-52::[URA3 GAL1p-SEC15; pNB304]/ura3-52; leu2-3,112 leu2-3,112 GAL+*
NY2145	*MAT**a** sec2-Δ1::HIS3 leu2-3,112::[LEU2 SEC2;pNB977] his3-Δ200 ura3-52 GAL+*
NY2146	*MAT**a** sec2-Δ1::HIS3 leu2-3,112::[LEU2 SEC2-GFP;pNB985] his3-Δ200 ura3-52 GAL+*
NY2147	*MAT**a** sec2-Δ1::HIS3 leu2-3,112::[LEU2 sec2-59-GFP;pNB990] his3-Δ200 ura3-52 GAL+*
NY2152	*MAT**a** sec2-Δ1::HIS3 leu2-3,112::[LEU2 sec2-78-GFP;pNB991] his3-Δ200 ura3-52 GAL+*
NY2432	*MATα leu2-3,112::[LEU2 GAL1p-GST-SEC2; pNB1153] ura3-52 pep4::URA3 GAL+*
NY2433	*MATα leu2-3,112::[LEU2 GAL1p-GST; pNB1154] ura3-52 pep4::URA3 GAL+*
NY2434	*MATα leu2-3,112::[LEU2 GAL1p-GST-sec2(aa.1-160); pNB1157] ura3-52 pep4::URA3 GAL+*
NY2435	*MATα leu2-3,112::[LEU2 GAL1p-GST-sec2-59(aa.1-374); pNB1155] ura3-52 pep4::URA3 GAL+*
NY2436	*MATα leu2-3,112::[LEU2 GAL1p-GST-sec2-70(aa.1-508); pNB1156] ura3-52 pep4::URA3 GAL+*
NY2437	*MATα leu2-3,112::[LEU2 GAL1p-GST-sec2(aa.161-759); pNB1159] ura3-52 pep4::URA3 GAL+*
NY2438	*MATα leu2-3,112::[LEU2 GAL1p-GST-sec2-78; pNB1160] ura3-52 pep4::URA3 GAL+*
NY2439	*MATα leu2-3,112::[LEU2 GAL1p-GST-sec2(aa.1-450); pNB1161] ura3-52 pep4::URA3 GAL+*
NY2440	*MAT**a** leu2-3,112 his3200 ura3-52 SEC3-GFP [URA] GAL+*
NY2441	*MAT**a** leu2-3,112 his3Δ200 ura3-52 SEC5-GFP [URA] GAL+*
NY2443	*MAT**a** leu2-3,112 his3Δ200 ura3-52 SEC8-GFP [URA] GAL+*
NY2446	*MAT**a** leu2-3,112 his3Δ200 ura3-52 EXO70-GFP [URA] GAL+*
NY2520	*MATα leu2-3,112::[LEU2 EXO70-TAP] his3−Δ200::[HIS3 SEC5-3×HA kanMX6] ura3-52 GAL+*
NY2522	*MATα leu2-3,112::[LEU2 GAL1p-GST-sec2(aa.1-258);pNB1236] ura3-52 pep4::URA3 GAL+*
NY2523	*MATα leu2-3,112::[LEU2 GAL1p-GST-sec2(aa.161-258);pNB1237] ura3-52 pep4::URA3 GAL+*
NY2524	*MATα leu2-3,112::[LEU2 GAL1p-GST-sec2(aa.161-374);pNB1238] ura3-52 pep4::URA3 GAL+*
NY2525	*MAT**a**/α ura3-52::[URA3 GAL1p-SEC15; pNB304])/ura3-52; leu2-3,112::[LEU2 GAL1p-GST-SEC2; pNB1153]/leu2-3,112 GAL+*
NY2526	*MAT**a**/α ura3-52::[URA3 GAL1p-SEC15]; pNB304]/ura3-52; leu2-3,112::[LEU2 GAL1p-GST-SEC10;pNB1239]/leu2-3,112 GAL+*
NY2527	*MAT**a**/α ura3-52::[URA3 GAL1p-SEC15]; pNB304]/ura3-52; leu2-3,112::[LEU2 GAL1p-GST; pNB1154]/leu2-3,112 GAL+*
NY2528	*MAT**a**/α ura3-52/ura3-52; leu2-3,112::[LEU2 GAL1p-GST-SEC2; pNB1153]/leu2-3,112 GAL+*
NY2529	*MAT**a**/α ura3-52/ura3-52; leu2-3,112::[LEU2 GAL1p-GST-SEC10; pNB1239]/leu2-3,112 GAL+*
NY2530	*MAT**a**/α ura3-52/ura3-52; leu2-3,112::[LEU2 GAL1p-GST; pNB1154]/leu2-3,112 GAL+*
NY2531	*MAT**a** ura3-52::[URA3 GAL1p-SEC15; pNB304]; leu2-3,112 GAL+*
NY2532	*MATα ura3-52::[URA3 GAL1p-SEC15; pNB304]; leu2-3,112::[LEU2 GAL1p-GST-SEC2; pNB1153] GAL+*
NY2533	*MATα ura3-52::[URA3 GAL1p-SEC15; pNB304]; leu2-3,112::[LEU2 GAL1p-GST-SEC10;pNB1239] GAL+*
NY2534	*MATα ura3-52::[URA3 GAL1p-SEC15; pNB304]; leu2-3,112::[LEU2 GAL1p-GST; pNB1154] GAL+*
NY2535	*MATα ura3-52::[URA3 GAL1p-SEC15; pNB304]; leu2-3,112::[LEU2 GAL1p-GST-sec2(aa.1-160); pNB1157] GAL+*
NY2536	*MATα ura3-52::[URA3 GAL1p-SEC15; pNB304]; leu2-3,112::[LEU2 GAL1p-GST-sec2-59(aa.1-374); pNB1155] GAL+*
NY2537	*MATα ura3-52::[URA3 GAL1p-SEC15; pNB304]; leu2-3,112::[LEU2 GAL1p-GST-sec2(aa.1-450); pNB1161] GAL+*
NY2538	*MATα ura3-52::[URA3 GAL1p-SEC15; pNB304]; leu2-3,112::[LEU2 GAL1p-GST-sec2-70(aa.1-508); pNB1156] GAL+*
NY2539	*MAT**a** ura3-52::[URA3 GAL1p-SEC15; pNB304]; leu2-3,112::[LEU2 GAL1p-GST-sec2(aa.161-759); pNB1159] GAL+*
NY2540	*MATα ura3-52::[URA3 GAL1p-SEC15; pNB304]; leu2-3,112::[LEU2 GAL1p-GST-sec2-78; pNB1160] GAL+*
NY2541	*MATα ura3-52::[URA3 GAL1p-SEC15; pNB304]; leu2-3,112::[LEU2 GAL1p-GST-sec2(aa.1-258);pNB1236]] GAL+*
NY2542	*MAT**a** ura3-52::[URA3 GAL1p-SEC15; pNB304]; leu2-3,112::[LEU2 GAL1p-GST-sec2(aa.161-258);pNB1237] GAL+*
NY2543	*MAT**a** ura3-52::[URA3 GAL1p-SEC15; pNB304]; leu2-3,112::[LEU2 GAL1p-GST-sec2(aa.161-374);pNB1238] GAL+*
NY2544	*MAT**a**/α ura3-52/ura3-52; leu2-3,112/leu2-3,112 his3/HIS3 GAL+*
NY2545	*MATα ura3-52 leu2-3,112 his3 Sec15-13×myc kanMX6 GAL+*
NY2546	*MAT**a** sec2-Δ1::HIS3 ura3-52 leu2-3,112::[LEU2 SEC2; pNB977] his3 Sec15-13×myc kanMX6 GAL+*
NY2547	*MAT**a** sec2-Δ1::HIS3 ura3-52 leu2-3,112::[LEU2 SEC2-GFP; pNB985] his3 Sec15-13×myc kanMX6 GAL+*
NY2548	*MAT**a** sec2-Δ1::HIS3 ura3-52 leu2-3,112::[LEU2 sec2-59-GFP;pNB990] his3 Sec15-13×myc kanMX6 GAL+*
NY2549	*MAT**a** sec2-Δ1::HIS3 ura3-52 leu2-3,112::[LEU2 sec2-78-GFP;pNB991] his3Sec15-13×myc kanMX6 GAL+*
NY2550	*MAT**a**/α ura3-52::[URA3 GAL1p-SEC6;pNB1240])/ura3-52; leu2-3,112::[LEU2 GAL1p-GST-SEC2; pNB1153]/leu2-3,112 GAL+*
NY2551	*MAT**a**/α ura3-52::[URA3 GAL1p-SEC6;pNB1240]/ura3-52; leu2-3,112::[LEU2 GAL1p-GST-SEC10;pNB1239]/leu2-3,112 GAL+*
NY2552	*MAT**a**/α ura3-52::[URA3 GAL1p-SEC6;pNB1240]/ura3-52; leu2-3,112::[LEU2 GAL1p-GST; pNB1154]/leu2-3,112 GAL+*
NY2586	*MAT sec2-Δ1::HIS3 leu2-3,112::[LEU2 SEC2-GFP; pNB985] his3 ura3-52::[URA3 GAL1p-SEC15] GAL+*
SFNY1311	*MAT**a** ura3-52 leu2-3,112, his3-Δ200::[HIS GAL1p GST-GEA2]*
SFNY1586	*MAT**a** ura3-1 leu2-3,112 trp1-1 ade2-1 can1-100 VPS1::[GAL1p GST-VPS1, HIS3]*
NY2638	*MATα leu2-3,112 his3Δ200 ura3-52 SEC3-GFP [URA] sec2-59 GAL+*
NY2639	*MAT his3Δ200 ura3-52 SEC5-GFP [URA] sec2-59 GAL+*
NY2640	*MAT leu2-3,112 ura3-52 SEC8-GFP [URA] sec2-59 GAL+*
NY2641	*MATα leu2-3,112 his3Δ200 ura3-52 EXO70-GFP [URA] sec2-59 GAL+*
NY2642	*MAT sec2-Δ1::HIS3 ura3-52 leu2-3,112::[LEU2 SEC2-GFP; pNB985] his3 Sec15-13×myc kanMX6 elp1Δ kanMX6 GAL+*
NY2643	*MAT sec2-Δ1::HIS3 ura3-52 leu2-3,112::[LEU2 sec2-59-GFP;pNB990] his3 Sec15-13×myc kanMX6 elp1Δ kanMX6 GAL+*
NY2644	*MAT sec2-Δ1::HIS3 ura3-52 leu2-3,112::[LEU2 sec2-78-GFP;pNB991] his3 Sec15-13×myc kanMX6 elp1Δ kanMX6 GAL+*
NY2645	*MAT**a** sec2-Δ1::HIS3 leu2-3,112::[LEU2 sec2-59-GFP;pNB990] his3-Δ200 ura3-52 elp1Δ kanMX6 GAL+*
NY2646	*MATα sec2-Δ1::HIS3 ura3-52 leu2-3,112::[LEU2 SEC2-GFP; pNB985] his3 Sec15-13×myc kanMX6 sec5-24 GAL+*

Iodixanol Gradient Centrifugation

Spheroplasted cells (200 OD$_{600}$ units) were lysed in a buffer containing 20 mM TEA-acetate, pH 7.2, 0.8 M sorbitol, 1 mM EDTA, and protease inhibitors. Lysates were spun at $10,000 \times g$ for 10 min at 4°C. To stabilize Sec15p-membrane association, 1 M 2-(*N*-morpholino)ethanesulfonic acid (MES), pH 6.5, was added to the cleared lysates to reach a final concentration of 50 mM. Then, 100 μl of pH-adjusted lysates were mixed with 0.4 ml of 50% iodixanol, 20 mM TEA-acetate, pH 7.2, 0.4 M sorbitol, and 1 mM EDTA, so that the final
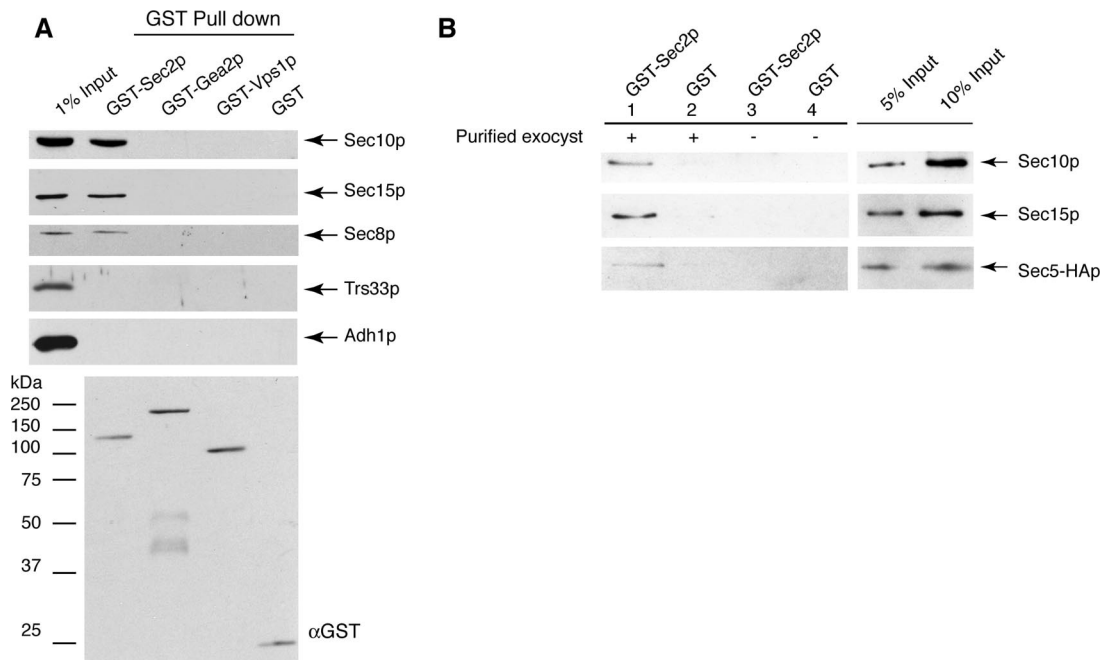
Figure 1. Interaction between Sec2p and the exocyst. (A) Exocyst subunits are present in GST-Sec2p pull downs from yeast. To induce expression of GST-Sec2p (NY2432), GST-Gea2p (SFNY1311), GST-Vps1p (SFNY 1586), and GST (NY2433), the cells were grown in YP medium containing 2% galactose. GST pull downs were carried out as described in *Materials and Methods*. The efficiency of GST-Sec2p, GST-Gea2p, and GST-Vps1p pull downs was 40–50%, whereas the efficiency of GST pull down was 90%. Western blots were probed with αSec10p, αSec15p, αSec8p, αTrs33p, and αAdhp. The relative amount of GST-fusion protein in the pull downs assessed by blotting with αGST. The input represents 1% of lysate prepared from yeast strain NY2432. Lysates from all strains used in this experiment were adjusted to the same protein concentration before pull downs. The amounts of Sec8p, Sec10p, Sec15p, Trs33p, and Adhp were equal in these lysates and corresponded to the endogenous amount present in a wild-type strain. (B) Purified GST-Sec2p interacts with purified exocyst in vitro. GST-Sec2p (purified from NY2432) immobilized on glutathione-Sepharose beads (20 μl of 50% slurry of beads, the estimated amount of GST-Sec2p is 0.5 μg) was incubated for 1 h at room temperature with intact exocyst complex purified from NY2520 (lane 1) in a buffer containing 20 mM PIPES, pH 6.8, 150 mM NaCl, 0.5 mg/ml BSA, 1 mM magnesium acetate, 1 mM imidazole, 2 mM CaCl$_2$, 0.1% Igepal 30, and 10 mM 2-mercaptoethanol in a total volume of 200 μl. The purification of the exocyst is described in *Materials and Methods*. The control (lane 2) represents exocyst binding to the GST protein immobilized on glutathione-Sepharose beads. The amount of endogenous exocyst copurifying with GST-Sec2p or GST from yeast (lanes 3 and 4) is negligible compared with the amount of purified exocyst added to the binding mixtures. The input represents 5 and 10% of the purified exocyst used in the binding mixtures. The exocyst subunits, Sec10p and Sec15p were detected with αSec10p and αSec15p antibody, respectively. Sec5-HA fusion protein was detected with αHA antibody. The results shown represent one of three independent experiments.

concentration of iodixanol was 40%. The mixture (0.1 ml) was loaded to the bottom of an 11 × 34-mm polycarbonate tube (Beckman Coulter) underneath 1 ml of 35% iodixanol, 20 mM TEA-acetate, 20 mM MES, pH 6.8, 0.4 M sorbitol, and 1 mM EDTA. The tubes were centrifuged in a TLA 120.2 rotor at 100,000 × *g* for 3 h. Fractions of 150 μl were taken from the top. Then, 120 μl of each fraction was mixed with 0.5 ml of 20 mM HEPES, pH 7.0, 120 mM NaCl, 1 mM EDTA, and 1% TX-100 and subjected to immunoprecipitation with anti-GFP antibody. Sec15-13xmycp in the immunoprecipitates was detected by anti-myc.

Sorbitol Gradients

An 11-ml linear 20–40% sorbitol gradient in 20 mM TEA-acetate, 10 mM MES, pH 6.8, and 1 mM EDTA was prepared as described previously (Brennwald *et al.*, 1994). The cells were lysed and spheroplasted, and the resulting lysate was spun at 10,000 × *g* for 10 min to obtain S10. S10 supernatant (0.6 ml; equivalent to ~60 OD$_{600}$) was layered on top of the gradient and centrifuged in a SW41 rotor at 38,000 rpm for 2 h 20 min at 4°C and then fractionated (800-μl fractions). A portion of each gradient fraction was boiled in SDS sample buffer and analyzed by SDS-PAGE and immunodetection. Latent Kex2p and invertase activity in each fraction was measured as described previously (Walworth and Novick, 1987; Cunningham and Wickner, 1989). Then, 600 μl of each fraction was subjected to immunoprecipitation with αGFP. Before immunoprecipitation, TX-100 and Tris, pH 8.0, were added to reach the final concentration, 1% and 20 mM, respectively. Sec15-13xmycp in the immunoprecipitates was detected with anti-myc.

Fluorescence Microscopy

For GFP visualization, cells were examined with a Zeiss Axioplan2 upright fluorescence microscope by using a 63× Plan Neofluor apochromatic oil-immersion objective with numerical aperture 1.3. Images were captured with a Hammamatsu ORCA ER cooled charge-coupled device camera and analyzed with Open lab software from Improvision (Lexington, MA).

RESULTS

Exocyst Subunits Are Present in GST-Sec2p Pull Downs from Yeast

To determine whether Sec2p interacts with the exocyst, we expressed GST N-terminally tagged Sec2p in yeast under the control of the strong *GAL1* promoter and performed GST-Sec2p pull downs. GST-Sec2p is fully functional in vivo (Ortiz *et al.*, 2002). As shown in Figure 1A, exocyst complex subunits Sec10p, Sec15p, and Sec8p were identified in GST-Sec2p pull downs from yeast. Very low or undetectable levels of exocyst components were found in control pull downs with GST protein alone or with GST-Gea2p and GST-Vps1p. Gea2p is an exchange factor for the Arf GTPase, whereas Vps1 is a member of the dynamin GTPase family. All the GST fusion proteins were expressed and purified at similar levels. As a control for nonspecific binding, we have also blotted for Trs33p, a subunit of the TRAPP tethering complex that functions in endoplasmic reticulum (ER)-Golgi transport and Adh1p, a cytosolic marker.
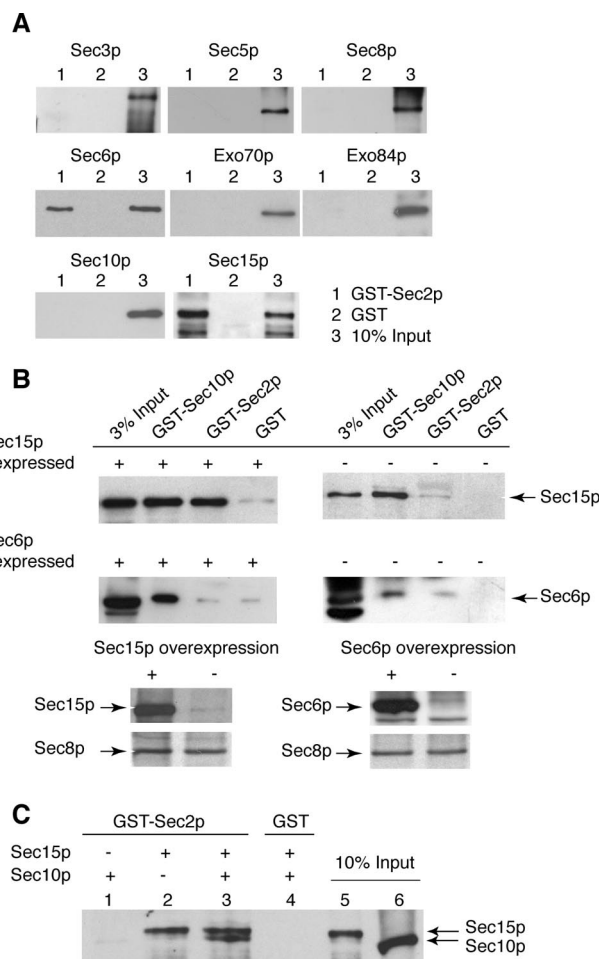
Sec2p Directly Interacts with the Exocyst Complex

To determine whether the interaction between Sec2p and the exocyst is direct, we performed in vitro binding experiments with purified proteins (Figure 1B). For these experiments, GST-Sec2p and the intact, TAP-tagged exocyst complex were independently purified from yeast. In the binding experiments, GST-Sec2p attached to glutathione-Sepharose beads was incubated with purified exocyst complex. As shown previously, purified exocyst contained approximately equimolar amounts of all eight subunits, which was confirmed by silver staining of SDS-PAGE gel (TerBush *et al.*, 1996). GST alone bound to beads was used as a control for nonspecific binding. There was a small amount of endogenous exocyst copurifying with GST-Sec2p from yeast (Figure 1A), but the amount of purified exocyst bound to GST-Sec2p beads in these binding experiments (Figure 1B) was several-fold higher. About 5% of the exocyst input specifically bound to GST-Sec2p (lane 1). Similar percentages of Sec10p, Sec15p, Sec5-3xHAp (Figure 1B), Sec8p, and Sec6p (our unpublished data) coprecipitated with GST-Sec2p. Previous studies on exocyst assembly have shown, that in *sec5-24*, *sec3-2* and *sec10-2* mutants, the exocyst complex is largely disrupted (TerBush *et al.*, 1996). Hence, the fact that Sec5p and Sec10p are precipitated with similar efficiency as the other subunits in the GST-Sec2p binding assay leads us to conclude that the intact exocyst complex is able to interact with Sec2p. Similar results were obtained when GST-Sec2p purified from *E. coli* was used for these binding experiments (our unpublished data).

## The Sec15p Subunit of the Exocyst Complex Binds Sec2p

To determine which subunit within the Exocyst complex binds to Sec2p, we individually expressed in bacteria and purified all exocyst subunits (Sec3p, Sec5p, Sec6p, Sec8p, Sec10p, Sec15p, Exo70p, and Exo84p) and used these isolated subunits for in vitro binding studies with bacterial GST-Sec2p (Figure 2A). In this experiment, two exocyst subunits, Sec15p and Sec6p, showed significant binding, suggesting that the Sec2p–exocyst complex interaction could occur through either or possibly both of these subunits.

To further explore the Sec2p–Sec15p and Sec2p–Sec6p interactions in yeast, we co-overexpressed GST-Sec2p with either Sec15p or Sec6p in yeast. The level of Sec15p and Sec6p overexpression (20-fold) was similar to the level of GST-Sec2p overexpression. On co-overexpression of Sec15p and GST-Sec2p, a significantly larger amount of Sec15p was pulled down with GST-Sec2p compared with a pull down from the corresponding strain expressing normal levels of Sec15p (Figure 2B, top). Because all other exocyst subunits are present at endogenous levels, this result is consistent with the hypothesis that Sec15p directly binds Sec2p without any intermediary proteins. GST-tagged Sec10p was used as a positive control as Sec10p has been shown to be a direct interacting partner of Sec15p within the exocyst complex (Guo *et al.*, 1999). A relatively small amount of Sec15p is present in GST-Sec2p pull downs compared with GST-Sec10p pull downs when Sec15p is at native levels. However, upon Sec15p overexpression the amount of Sec15p in GST-Sec2p and GST-Sec10p pull downs is comparable.

On co-overexpression of GST-Sec2p and Sec6p, only a background level of Sec6p was present in the GST-Sec2p pull downs (Figure 2B, bottom). In contrast, upon co-overexpression of GST-Sec10p and Sec6p, an increased amount of Sec6p was found in the GST-Sec10p pull down. Thus, we were unable to confirm the results from our binding studies in which we used recombinant Sec6p purified from bacteria

Figure 2. The Sec15p subunit of the exocyst complex interacts with GST-Sec2p. (A) Full-length GST-Sec2p was purified from *E. coli* strain BL21. As a control, GST protein was also purified from *E. coli*. GST-Sec2p (lanes 1) and GST (lanes 2) immobilized on glutathione-Sepharose beads (20 μl of 50% slurry, the amount of the fusion protein on beads is 2.5 μg) were incubated with the different exocyst subunits (0.5 μg) individually purified from *E. coli*. The binding reaction was performed in a buffer containing 1× PBS, 1 mg/ml BSA, and 0.25% Triton X-100 for 1 h at room temperature. Lanes 3 represents 10% of the input of each individually purified exocyst subunit. His$_6$-exocyst subunits were detected with monoclonal αHis (Novagen). (B) Co-overexpression of GST-Sec2p and Sec15p in yeast results in increased coprecipitation of Sec15p with GST-Sec2p. Top left, GST-Sec2p was co-overexpressed with Sec15p in yeast (NY2525) and isolated using glutathione-Sepharose beads. As a control GST-Sec10p (a known Sec15p interacting protein; positive control) and GST (negative control) were also co-overexpressed with Sec15p (NY2526 and NY2527, respectively). Top right, similar GST pull downs, except that the amount of Sec15p is at native level (NY2528, NY2529, and NY2530). In the Sec15p-overexpressing yeast strains, the amount of Sec15p is 20-fold higher than native amount. Middle, this experiment was analogous to the top experiment, except that in this case, Sec6p was co-overexpressed with GST-Sec2p (NY2550), GST-Sec10p (NY2551), and GST (NY 2552). The exposure times for left and right panels are different. Bottom, amount of Sec15p and Sec6p in overproducing and nonoverproducing yeast lysates. Sec8p is shown as a loading control. In all these experiments, cells were grown overnight in YP + 2% glycerol and induced by adding 2% galactose for 8 h. (C) Binding sites for Sec2p and Sec10p on Sec15p are nonoverlapping. GST-Sec2p immobilized on glutathione beads was incubated with Sec10p (lane 1), Sec15p (lane 2), or both (lane3). Control binding to GST is shown in lane 4. All proteins were expressed and purified from bacteria. The binding reaction was performed as in A. Lanes 5 and 6 represent 10% of input of Sec15p and Sec10p, respectively.
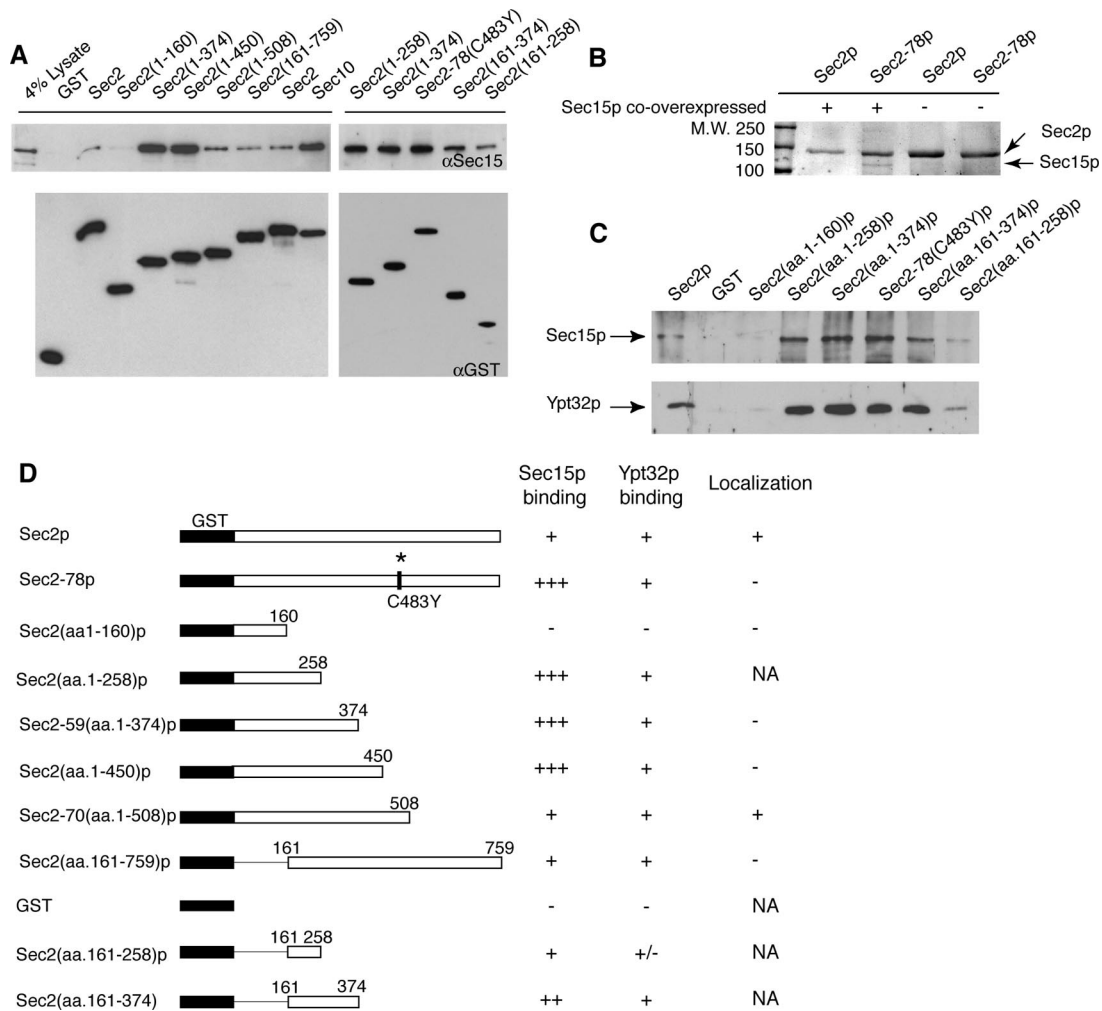
Figure 3. The Sec15p binding site is on the N-terminal half of Sec2p, whereas the "localization domain" (aa.451-508) is inhibitory to binding. (A) Sec2p constructs N-terminally tagged with GST were co-overexpressed with Sec15p (NY2532-2543). Cells were grown overnight in YP + 2% glycerol and induced by adding 2% galactose for 8 h. Fusion proteins were pulled down using glutathione-Sepharose beads as described in *Materials and Methods*, and the Sec15p present in these pull downs was detected with αSec15p antibody. For a loading control, GST-Sec2p constructs were detected by αGST antibody. (B) Sec2p and Sec2-78p N-terminally tagged with GST were overexpressed in yeast with (NY2532 and NY2540) or without (NY2432 and NY2438) concurrent overexpression of Sec15p. Complex formation between Sec2-78p and Sec15p (lane 2) can be detected by staining SDS-PAGE gels with Coomassie brilliant blue. (C) The binding sites for Sec15p and Ypt32p on Sec2p overlap. GST-Sec2p constructs were purified from yeast strains (NY2432-2439 and NY2522-2524) using glutathione-Sepharose beads. Binding studies with recombinant His$_6$-Ypt32p and His$_6$-Sec15p purified from *E. coli* were performed as described in *Materials and Methods*. Ypt32p was preloaded with GTPγS. His$_6$-Sec15p and His$_6$-Ypt32p were detected with αSec15p and αYpt32p antibodies, respectively. (D) Summary of Sec15p and Ypt32p binding to Sec2p constructs.

(Figure 2A) and have therefore pursued the interaction between Sec2p and Sec15p.

The data in Figure 1B suggested that the assembled exocyst interacts with Sec2p. If the Sec2p–exocyst interaction were mediated by the Sec15p subunit, it would be expected that both Sec2p and Sec10p (a direct Sec15p binding partner within the exocyst complex) could bind Sec15p at the same time. As shown in Figure 2C, Sec10p did not associate with GST-Sec2p alone; however, Sec10p was identified in the GST-Sec2p pull down when both Sec10p and Sec15p were included in the binding assay. These data indicate that Sec10p only interacts with Sec2p via Sec15p and implies that the binding sites for Sec10p and Sec2p on Sec15p are non-overlapping. A recent study has shown that the Sec10p binding site on Sec15p is located at the N terminus of Sec15p (France *et al.*, 2006). Our results (Figure 5C) suggest that the

Sec2p binding site on Sec15p is located at the C terminus of Sec15p.

Sec15p Binds to the N-Terminal Half of Sec2p; the C-Terminal Half of Sec2p Is Inhibitory to Binding

To define the Sec15p binding site on Sec2p, GST-tagged Sec2p truncations were co-overexpressed with Sec15p in yeast (for schematic diagram of Sec2p constructs, see Figure 3D) and retrieved on glutathione beads. As shown in Figure 3A, the Sec15p binding site on Sec2p is located within the N-terminal half of Sec2p. Sec15p shows little binding to the exchange domain (aa.1-160; Sec4p binding site), but it binds well to GST-Sec2(aa.1-258). As we examined longer constructs an additional effect became apparent. Sec15p binding to C-terminal truncations (GST-Sec2 aa.1-258, 1-374, and 1-450) as well as to a point mutant, GST-Sec2-78p, was
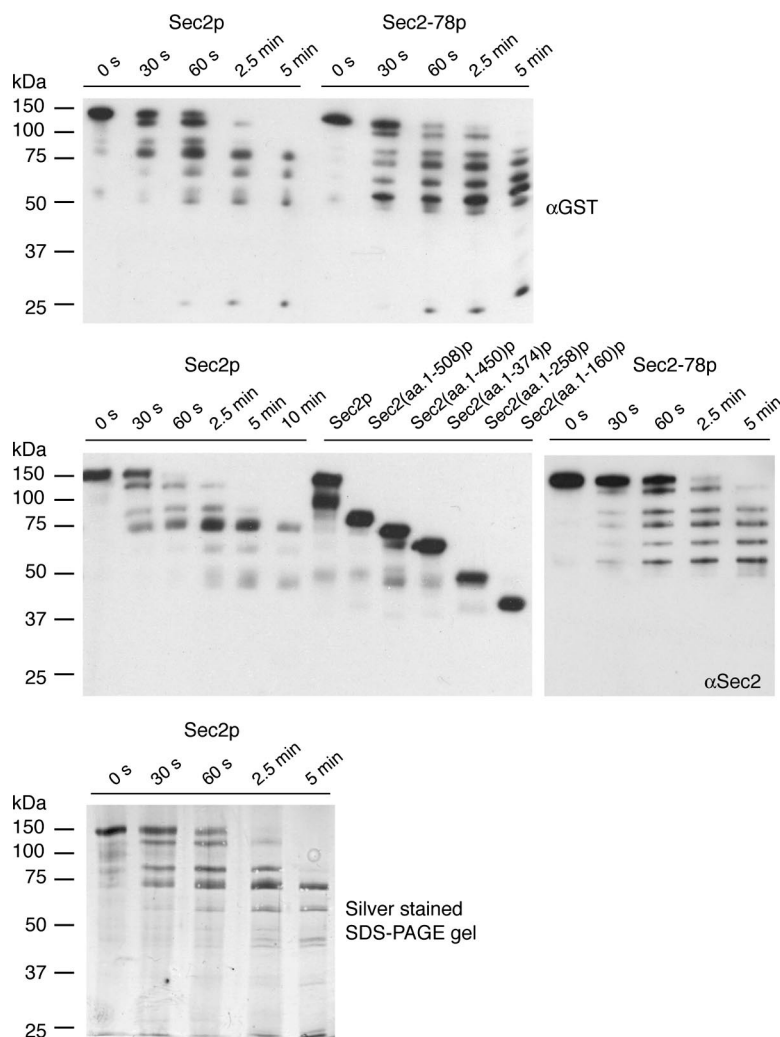
Figure 4. Limited proteolysis patterns for Sec2p and Sec2-78p purified from yeast (NY2432 and NY2438, respectively) are different. Trypsin digestion was allowed to proceed for 5 min, aliquots were withdrawn at t = 0 s, 30 s, 60 s, 2.5 min, and 5 min. Proteolytic fragments were detected with αGST (top) and αSec2p (middle) antibodies and by silver staining of an SDS-PAGE gel (bottom). Both antibodies recognize the N-terminal part of GST-Sec2p and show the same pattern. GST-Sec2 truncated proteins purified from yeast were included (middle) for size comparison with the proteolytic fragments.

15-fold more efficient than binding to wild-type GST-Sec2p. Indeed, the efficiency of Sec15p binding to these constructs was higher than the efficiency of Sec15p binding to GST-Sec10p (Figure 3A), and in these pull downs, Sec15p can be readily visualized by staining of SDS-PAGE gels with Coomassie brilliant blue (Figure 3B). One possible interpretation is that in these Sec2p truncations the binding site for Sec15p is more accessible than in full-length Sec2p. Importantly, the addition of only 58 amino acids to GST-Sec2(aa.1-450)p as in GST-Sec2-70(aa.1-508)p results in a dramatic reduction in the amount of coprecipitating Sec15p to the level present in a wild type GST-Sec2p pull down. Thus, the Sec2p region between amino acids 450 and 508 seems to be strongly inhibitory to Sec15p binding. The *sec2-78* point mutation (C483Y) also increases the efficiency of binding and lies within this region. This is precisely the same region that was previously shown to be necessary but not sufficient for proper localization of Sec2p (Elkind *et al.*, 2000; Figure 3D).

To further map the Sec15p binding site on Sec2p, we performed pull downs with two additional constructs, GST-Sec2(aa.161-258)p and GST-Sec2(aa.161-374)p. Sec15p is present in both pull downs but not nearly to the extent as in corresponding constructs containing the intact exchange domain, GST-Sec2(aa.1-258)p and GST-Sec2(aa.1-374)p. The smallest Sec2p fragment that still binds to Sec15p with high efficiency is 258 amino acids long [GST-Sec2(aa.1-258)p].

However when this region is divided further into the exchange domain GST-Sec2(aa.1-160)p and the region downstream from the exchange domain GST-Sec2(aa.161-258)p, this increased Sec15p binding is lost. We believe that the exchange domain is properly folded, because Sec4p binds efficiently to this construct. However, it is possible that the region immediately downstream (aa.161-258)p cannot properly fold in the absence of the exchange domain. It is also possible that the binding site for Sec15p includes part of the exchange domain along with the region immediately downstream.

The Ypt32p binding site on Sec2p was previously mapped to the region between amino acids 161 and 374. To narrow down this region and to compare Ypt32p binding to Sec15p binding, we performed additional binding experiments with newly constructed GST-Sec2p proteins. As shown in Figure 3C, Sec15p and Ypt32p binding to Sec2p display similar patterns, suggesting that in both cases the majority of binding determinants are located between amino acids 161-258 of Sec2p.

Sec2-78p Exists in a Conformational State Different from Wild-Type Sec2p

To explain the increased Sec15p binding efficiency seen with Sec2p truncations as well as the point mutant Sec2-78p, we
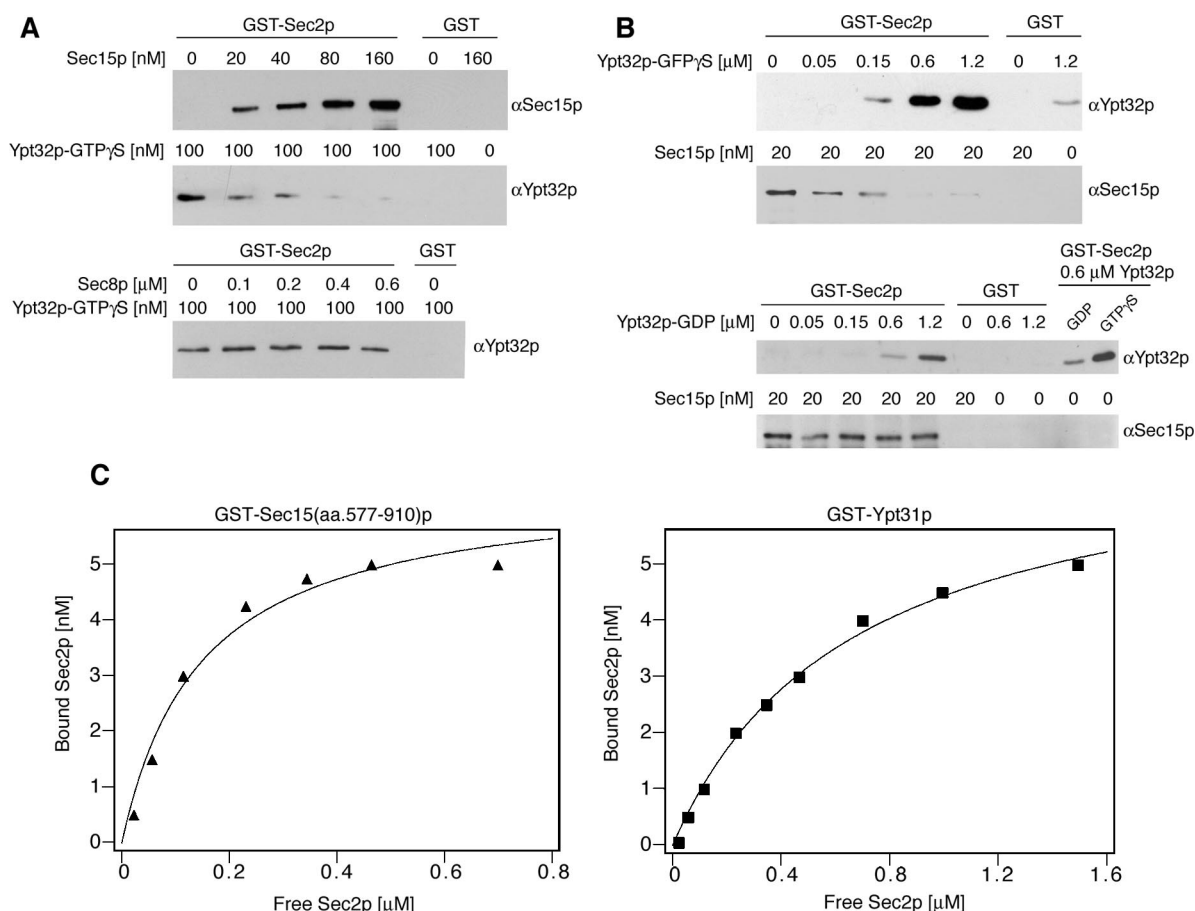
Figure 5. Sec15p and Ypt32p compete for binding to Sec2p. (A) GST-Sec2p or GST was immobilized on glutathione-Sepharose beads (20 μl of 50% slurry, the amount of the fusion protein on beads was 2.5 μg) and incubated with 100 nM His$_6$-Ypt32p preloaded with GTPγS as described previously (Ortiz *et al.*, 2002). Increasing amounts of His$_6$-Sec15p (top) or for a control His$_6$-Sec8p (bottom) were included in the binding mixtures. The binding reaction was performed in a buffer containing 1$\times$ PBS, 1 mg/ml BSA, and 0.25% Triton X-100 for 1 h at room temperature. (B) Top, GST-Sec2p or GST immobilized on glutathione-Sepharose beads was incubated with 20 nM His$_6$-Sec15p and increasing amounts of His$_6$-Ypt32p-GTPγS. Bottom, GDP-loaded Ypt32p binds GST-Sec2p less efficiently and does not displace Sec15p from GST-Sec2p. All proteins in this experiment were purified from *E. coli*. His$_6$-Sec15p and His$_6$-Ypt32p were detected with αSec15p and αYpt32p antibodies, respectively. (C) The relative affinities of Sec2p-Ypt31p and Sec2-Sec15p interactions. GST-Ypt31p, GST-Sec15(aa.577-910)p and His$_6$-Sec2p were purified from *E. coli* by using glutathione-Sepharose and Ni-NTA agarose, respectively. Various amounts of His$_6$-Sec2p were incubated with 20 nM GST-Ypt31p, GST-Sec15(aa.577-910)p, or GST attached to glutathione-Sepharose beads in a total volume 100 μl for 60 min at room temperature. GST-Ypt31p was preloaded with GTPγS, and no binding was observed for the nucleotide free or GDP bound forms of GST-Ypt31p. The protein samples were subjected to SDS-PAGE, and the amount of bound His$_6$-Sec2p was determined by Western blotting with αSec2p antibody. Bound His$_6$-Sec2p was plotted against free His$_6$-Sec2p and the dissociation constant K_d was estimated by fitting the results with a single rectangular hyperbola equation: $B = B_{max}L/(K_d + L)$, where B is bound and L is free His$_6$-Sec2p. Three independent experiments estimated the dissociation constant K_d of GST–Ypt31p–Sec2p interaction to be 0.65 $\pm$ 0.1 μM, whereas the K_d of the GST-Sec15(aa.577-910)p–Sec2p interaction was 0.15 $\pm$ 0.05 μM.

propose that in these proteins the binding site for Sec15p is more accessible than in wild-type full-length Sec2p. To test this hypothesis, we subjected GST-Sec2p and GST-Sec2-78p purified from yeast to limited tryptic digestion. As shown in Figure 4 (top), the proteolytic pattern of these two proteins differs significantly. The digestion pattern observed by silver staining of an SDS-PAGE gel (Figure 4, bottom) is similar to the pattern observed by Western blotting with αGST and αSec2 antibodies, suggesting that Sec2p is degraded from the C terminus. A relatively stable intermediate, ending at a site between 451 and 508 amino acids from the N terminus, accumulates in the GST-Sec2p digest but not in GST-Sec2-78p digest (Figure 4, middle). It is important to note, that the Sec2p region 451–508 is important for both localization and regulation of Sec15p binding. Sec2-78p is quickly degraded beyond this region, stalling when the fragment is ~258

amino acids long. Thus, the greater accessibility of GST-Sec2-78p to trypsin supports the hypothesis that the mutant Sec2-78p exists in a more open conformation.

Ypt32p and Sec15p Compete for Binding on Sec2p

The Sec15p and Ypt32p binding sites on Sec2p were not resolved by deletion analysis, suggesting that they might be overlapping. We therefore performed competition experiments with recombinant proteins purified from *E. coli*. As shown in Figure 5A, Sec15p in the concentration range of 20–80 nM can largely compete Ypt32p binding on Sec2p. Similarly, activated Ypt32p, in the concentration range of 50–600 nM, can substantially compete Sec15p binding on Sec2p (Figure 5B). Sec8p does not compete Ypt32p binding (Figure 5A) and Ypt32p in its GDP-bound form does not compete Sec15p binding (Figure 5B).

To assess the relative affinities of the Sec2p–Sec15p interaction and the Sec2p–Ypt31/32p interaction, we performed binding reactions with GST-Ypt31-GTPp or GST-Sec15(aa.577-910)p attached to glutathione-Sepharose beads and varying amounts of purified His$_6$-Sec2p. GST-Ypt31p was used in this experiment because of the difficulty of expressing and purifying large amounts of soluble GST-Ypt32p. We were also unable to purify large amounts of full length GST-Sec15p. However, we were able to obtain workable amounts of a GST-tagged C-terminal fragment of Sec15p comprised of amino acids 577-910 and found that this construct binds Sec2p efficiently. As shown in Figure 5C, GST-Ypt31p binds Sec2p with lower relative affinity compared with GST-Sec15(aa.577-910)p. Three independent experiments estimated the dissociation constant K_d of GST-Ypt31p-Sec2p interaction to be 0.65 ± 0.1 μM, whereas the K_d of the GST-Sec15(aa.577-910)p–Sec2p interaction was 0.15 ± 0.05 μM.

The Microsomal Pool of Sec2p Interacts with the Exocyst

To determine whether Sec2p and the exocyst interact at normal levels of expression, and if so, where this interaction occurs, we constructed a strain in which the sole copy of Sec2p is C-terminally tagged with GFP and the sole copy of Sec15p is C-terminally tagged with 13xmyc. Differential centrifugation was performed on lysates before immunoprecipitation of Sec2-GFP with αGFP antibody. These immunoprecipitates were then probed with αmyc antibody to detect Sec15p. Previous studies showed that full-length Sec2p is present in a greater amount in the 100,000 × g supernatant (S100) than in the 100,000 × g pellet (P100) (Elkind *et al.*, 2000). As shown in Figure 6 (lanes 1 and 2), Sec15p can be readily coimmunoprecipitated with Sec2p from solubilized P100, representing the microsomal pellet containing post-Golgi vesicles and other small cellular components. Little specific Sec15p can be found in immunoprecipitates from S100, where the majority of Sec2p is present.

Increased Association of Mutant Sec2 Proteins with the Exocyst Parallels Their Mislocalization In Vivo

Previous studies (Elkind *et al.*, 2000) showed that mutated Sec2 proteins, such as *sec2-59* or *sec2-78* are shifted in their distribution from S100 to P100 and that this shift in distribution correlated with the loss of polarized localization of the corresponding GFP-tagged proteins (Supplemental Figure 1). Flotation gradients established that this redistribution to P100 was not due to tighter association with membranes, but rather that the mutant Sec2p formed a high-molecular-weight, proteinaceous complex or aggregate (Elkind *et al.*, 2000). To test the possibility that the redistribution of mutant Sec2 proteins into the microsomal pellet reflects their increased interaction with the exocyst, we performed fractionation followed by immunoprecipitation of yeast lysates expressing Sec2-59(aa.1-374)p-GFP and Sec2-78(C483Y)p-GFP. As shown in Figure 6 (lanes 3 and 4), the portion of mutant Sec2p that shifts into P100 indeed seems to interact with the exocyst, because the amount of Sec15p in these αGFP immunoprecipitates is significantly higher than the amount of Sec15p coimmunoprecipitating with wild-type Sec2p. In addition, even the soluble pool of mutant Sec2 proteins shows increased association with Sec15p. Thus, there is a strong correlation between the tendency of mutant Sec2 proteins to mislocalize in the cell and their increased association with the Sec15p subunit of the exocyst complex. We propose that the observed mislocalization of Sec2p mutants is due to this tighter interaction with the exocyst.

To further examine complex formation between Sec2p and the exocyst, we have performed velocity gradient fraction-
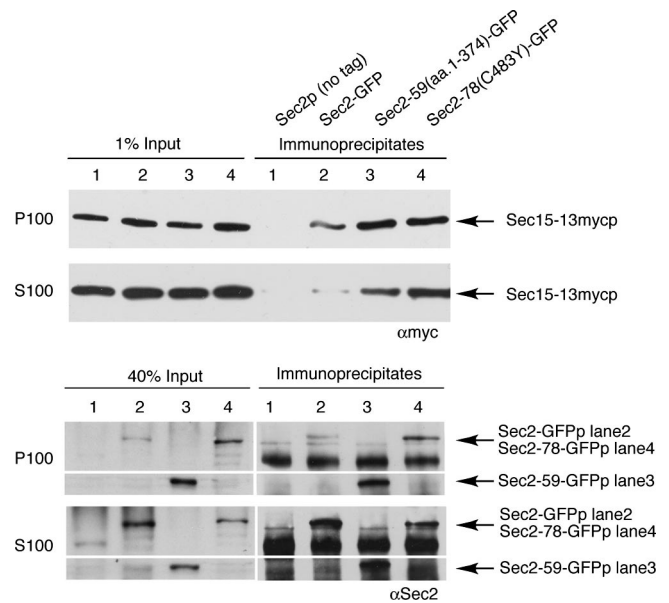
Figure 6. Sec15p is present in Sec2-GFPp immunoprecipitates from yeast. Top, Sec2-GFP was immunoprecipitated with αGFP (NY2547, lane 2) from both soluble (S100) and microsomal (P100) fractions. As a negative control, a yeast strain expressing untagged Sec2p was used (NY2546, lane 1). The amount of Sec15-13xmycp in the immunoprecipitates and 1% of input lanes was detected with αmyc. The experiment was conducted as described in *Materials and Methods*. The efficiency of the αGFP IP was 70–80% from S100 and 30–40% from P100. Immunoprecipitation of GFP-tagged Sec2p mutants Sec2-78-GFPp and Sec2-59-GFPp (NY2548 and NY2549, lanes 3 and 4) by using αGFP results in isolation of larger amounts of Sec15-13xmycp compared with Sec2-GFPp (lane 2). Bottom, amount of Sec2-GFPp (lane 2), Sec2-59-GFPp (lane 3), and Sec2-78-GFPp (lane 4) in the immunoprecipitates is consistent with the fact that in wild-type strain Sec2-GFPp is predominantly present in S100 fraction, whereas in mutant strains a portion of Sec2-59-GFPp and Sec2-78-GFPp redistributes from S100 to P100.

ation. In this experiment, yeast lysates solubilized with detergent were loaded onto a 10–35% glycerol gradient and centrifuged as described in *Materials and Methods*. This results in sedimentation of protein complexes according to their native size. As shown in Figure 7, A and B, Sec15p sediments similarly in both wild-type and *sec2-78* cells. The Sec15p peak coincided with that of Sec10p (Supplemental Figure 2) and Sec8p (our unpublished data) and corresponds to the assembled exocyst complex. In the wild-type strain, Sec2p sedimented more slowly than the exocyst with only a limited amount of overlap. In the *sec2-78* strain, the mutant Sec2-78p shifts toward a higher molecular weight, resulting in cosedimentation with the assembled exocyst complex. Portions of fractions 4–9 of each gradient were subjected to immunoprecipitation with αGFP antibody, and the immunoprecipitates were then probed with αmyc antibody to detect Sec15p. Approximately 1% of Sec15p can be immunoprecipitated with Sec2-GFPp from fractions 7, 8, and 9 (Figure 7A). These fractions correspond to the peak of the exocyst. A fivefold higher amount of Sec15p can be immunoprecipitated with Sec2-78-GFP from the equivalent fractions. No Sec15p was detected in the immunoprecipitates from a control strain expressing untagged Sec2p. Thus, the shift in Sec2-78p sedimentation seems to reflect its increased association with the exocyst complex. In these gradients, we have also examined sedimentation of Sec2p-interacting pro-
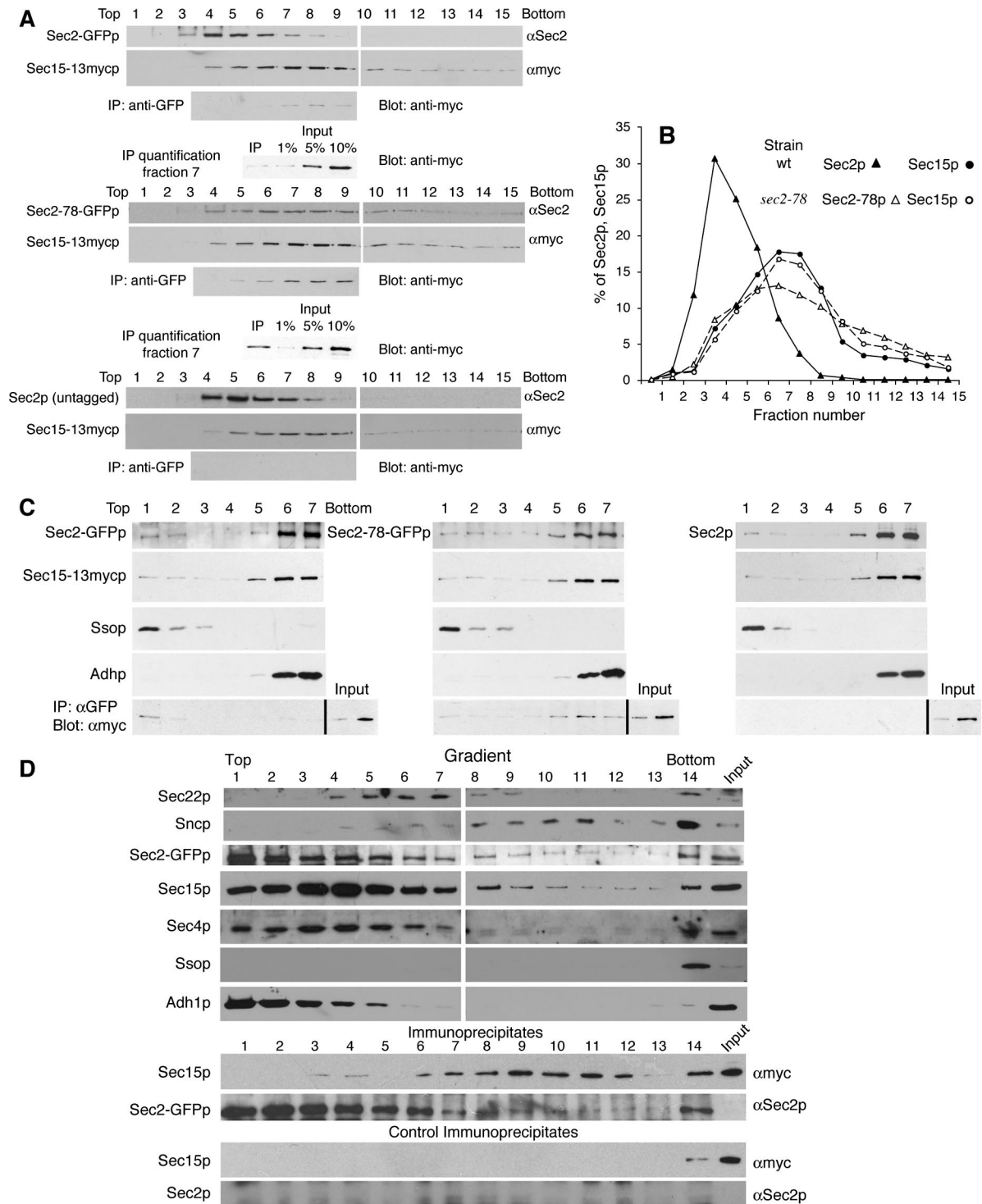
Figure 7. Velocity and density gradient analysis of Sec2p-exocyst binding. (A) NY2546 (Sec2p, Sec15-13xmycp), NY2547 (Sec2-GFPp, Sec15-13xmycp), and NY2549 (Sec2-78-GFPp, Sec15-13xmycp) lysates were subjected to velocity gradient centrifugation following detergent solubilization as described in *Materials and Methods*. Fifteen fractions were collected from the top and analyzed for the presence of Sec2p and Sec15p by Western blotting. From fractions 4 to 9, Sec2-GFPp was immunoprecipitated with anti-GFP, and Sec15-13xmycp present in the immunoprecipitations (IPs) was detected by anti-myc. One percent of Sec15p present in fractions 7, 8, and 9 can be coprecipitated with Sec2-GFPp; 5% of Sec15p present in fractions 7, 8, and 9 can be coprecipitated with Sec2-78-GFPp. No Sec15p was detected in the immunoprecipitates from the control strain containing untagged Sec2p. The efficiency of αGFP precipitation was typically 80%. (B) The sedimentation profiles of Sec2p and Sec15-13xmycp in wild-type (closed symbols) and *sec2-78* cells (open symbols) in 10–35% glycerol velocity gradients. (C) Precleared lysates of NY2547 (Sec2-GFPp, Sec15-13xmycp) and NY2549 (Sec2-78-GFPp, Sec15–13xmycp) and NY2546 (Sec2p, Sec15-13xmycp) were loaded at the bottom of a tube containing 35% iodixanol and centrifuged as described in *Materials and Methods*. Seven fractions were collected from the top. The amount of Sec2p, Sec15p, Ssop, and Adhp in each fraction was determined by Western blotting. The left panels show data for a strain expressing Sec2-GFPp (NY2547); the middle panels show data for a strain expressing

teins Sec4p and Ypt32p as well as other control proteins (Supplemental Figure 2). Sec4p and Ypt32p remain on top of these gradients in both wild-type and *sec2-78* cells.

Sec2p and the Exocyst Normally Associate on Membranes In Vivo

To examine where in the cell the Sec2p–Sec15p interaction occurs, we have used a floatation assay (Figure 7C). Yeast lysates prepared from strains expressing a single copy of Sec2-GFP or Sec2-78-GFP were supplemented with iodixanol to 40%, loaded beneath a layer of 35% iodixanol and centrifuged as described in *Materials and Methods*. Seven fractions were collected from the top. In this experiment, membranes and membrane-associated proteins float to the top of gradient, whereas cytosolic proteins remain where they were loaded at the bottom. The membrane markers Ssop (Figure 7C) and Sncp (our unpublished data) were found only in top fractions, whereas the cytosolic protein alcohol dehydrogenase (Adhp) remained at the bottom. As shown previously, the majority of Sec2p and Sec15p remained at the bottom; however, a small amount of these proteins floated up with the membrane fraction. We then performed immunoprecipitations from each fraction using anti-GFP antibody and probed for Sec15p in the immunoprecipitates (Figure 7C). In the strain expressing wild-type Sec2-GFP, Sec15p can be specifically coimmunoprecipitated only from the top (membrane) fractions, suggesting that the Sec2p–Sec15p interaction normally occurs on membranes (Figure 7C, bottom). This is despite the fact that the majority of Sec2p as well as Sec15p are found in the bottom (cytosolic) fractions. In the strain expressing Sec2-78-GFPp, the overall combined amount of Sec15p present in anti-GFP immunoprecipitates from all fractions is at least fivefold larger, and the coprecipitation of Sec15p is predominantly observed in the bottom fractions containing soluble Sec2-78-GFPp.

Our flotation gradients have shown that the Sec2p-Sec15p interaction normally occurs on membranes. To define the cellular compartment where this interaction takes place, subcellular fractionation was performed by velocity sedimentation through sorbitol gradients. In this experiment, the detergent-free cell lysates were first spun at $10,000 \times g$ to remove large membrane compartments such as most of the endoplasmic reticulum, mitochondria, and vacuoles as well as a large amount of plasma membrane, and then they were loaded on top of a 20–40% sorbitol gradient and centrifuged as described in *Materials and Methods*. After centrifugation, the positions of various membrane compartments within the gradient were determined by immunoblotting marker proteins or by enzymatic assays (Figure 7D). Sec22p, a SNARE that cycles between ER and Golgi, and Kex2p, a Golgi-localized protease, were selected as markers for the Golgi. The peak of Sec22p was in fractions 5–7 and corresponded to the peak of latent Kex2p activity (Supplemental Figure 3). The plasma membrane marker Ssop was found only at the bottom of the gradient. Sncp resides both on secretory vesicles and the plasma membrane and was found both at the bottom of the gradient and in fractions 8–11. The position of secretory vesicles under these gradient conditions was independently confirmed by repeating the fractionation with a *sec5-24* strain after a shift to 37°C to accumulate vesicles and assaying for latent invertase activity as well as immunoblotting for Sncp and Sec4p. It was shown previously that in *sec6-4* strain, Sec4p redistributes to secretory vesicles upon the shift to nonpermissive temperature (Goud *et al.*, 1988). In the *sec5-24* strain, the peaks of Sec4p, Sncp, and the invertase activity overlapped and corresponded to fractions 9–12 (Supplemental Figure 3). In the wild-type strain, only a small amount of Sec4p can be found in fractions that correspond to secretory vesicles (Figure 7D). We also examined the distribution of a cytosolic marker Adh1p and found it to remain in the top 5 fractions. The majority of Sec2p and Sec15p are also found in the top fractions; however, a small amount of each protein sediments further in the gradient. We then immunoprecipitated Sec2-GFPp, and for a negative control Sec2p, with αGFP from each gradient fraction and examined the amount of Sec15-13mycp in the immunoprecipitates. Sec15-13mycp is specifically found in the immunoprecipitates from gradient fractions 6–12, which is well separated from the large cytosolic pool of both proteins. By comparing the pattern of immunoprecipitations with that of different markers in the gradient, we conclude that the data are most consistent with the Sec2p–Sec15p interaction occurring on secretory vesicles.

Together, our study points to the exocyst as the partner of the mutant Sec2 proteins. Sec2p normally associates with the exocyst only while both are on secretory vesicles; however, mutant Sec2 proteins remain associated with the exocyst even after both are released to the cytosol. We propose that as a result of this tighter interaction with the exocyst, the mutant Sec2 proteins are unavailable to associate with a new round of vesicles, resulting in mislocalization.

Previous experiments showed that the overexpression of Sec15p in yeast results in a formation of a patch of Sec15p that colocalizes with a patch of Sec4p and a cluster of vesicles (Salminen and Novick, 1989). Because our results are most consistent with Sec2p–Sec15p interaction normally occurring on secretory vesicles, we have examined the localization of Sec2-GFP in a strain that overproduces Sec15p. Like Sec4p and Sec15p, under these conditions, Sec2-GFPp localized to a bright patch that is located either in the bud or adjacent to the emerging bud (Figure 8). This patch was previously shown to correspond to a cluster of secretory vesicles by thin section electron microscopy (Salminen and Novick, 1989).

Figure 7 (cont). Sec2-78-GFPp (NY2549). As a negative control, the identical experiment was also performed with a strain expressing untagged Sec2p (NY2546, right). For each fractionation experiment, a portion of each of the seven fractions was subjected to immunoprecipitation with anti-GFP and Sec15p was detected with anti-myc (bottom). The efficiency of αGFP precipitation was typically 70–80%. The input lane in all IP blots (bottom) represents 2.5% of Sec15-13xmycp present in fraction 1 (lane 8) and 2.5% of total Sec15-13xmycp in each lysate before the fractionation (lane 9). No Sec15-13xmycp was detected in a control αGFP precipitation from a strain expressing untagged Sec2p (NY2546). (D) Precleared lysates of NY2547(Sec2-GFPp, Sec15-13xmycp) and NY2546 (Sec2p, Sec15-13xmycp) were loaded on top of 20–40% sorbitol gradient and centrifuged as described in *Materials and Methods*. Fourteen fractions were collected from the top, and 2% of each fraction was analyzed for the amount of Sec22p, Sncp, Sec2p, Sec15p, Sec4p, Ssop, and Adh1p by Western blotting with an antibody raised against each protein except Sec15p, which was detected with αmyc. Input represents 0.14% of total protein loaded on top of the gradient. The distribution of markers upon fractionation of lysates prepared from strain NY2547 and a control strain NY2546 looked identical; therefore, only data for NY2547 are shown. A portion of each fraction was immunoprecipitated with αGFP, and the amount of Sec15-13mycp in the immunoprecipitates was determined with αmyc. Sec2-GFPp in the immunoprecipitates was detected with αSec2p. The input lane represents 0.05% of total protein loaded on top of the gradient. Control IPs represent identical immunoprecipitation experiments with the control strain NY2546 expressing untagged Sec2p.

DIC   FITC

Sec2-GFP

Sec2-GFP + GAL Sec15p
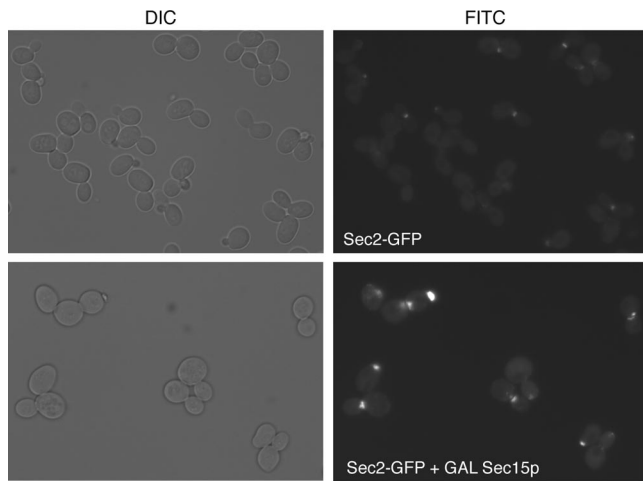
Figure 8. Localization of Sec2-GFPp in a strain overproducing Sec15p. Cells (NY2586) were grown at 25°C in YP-2% glycerol and then induced by adding 2% galactose for 15 h before visualization. Cells were examined with a Zeiss Axioplan2 upright fluorescence microscope as described in *Materials and Methods*.

DISCUSSION

Sec2p, like its substrate Sec4p, associates with secretory vesicles, and this association requires a stretch of 58 amino acids (aa.451-508) within the COOH-terminal half of Sec2p (Elkind *et al.*, 2000). Sec2p binds Ypt32-GTPp and overexpression of Ypt31/32p restores the localization of *sec2* alleles in which this region is lost or mutated. These data suggested a signal cascade model in which the activated upstream rabs, Ypt31/32p, act to position the GEF, Sec2p, which then activates Sec4p, the next rab GTPase along the pathway (Ortiz *et al.*, 2002). However, these studies did not define the function of the Sec2p localization region (aa.451-508).

Here, we show that Sec2p binds the exocyst complex through a direct interaction with Sec15p and that this interaction normally occurs on secretory vesicles. The Sec15p binding site on Sec2p overlaps with that of Ypt32p and the two proteins compete for binding to Sec2p. As an effector of Sec4p (Guo *et al.*, 1999), Sec15p not only binds the GEF that activates Sec4p but also responds to active Sec4p. Combining a GEF and effector in one complex may establish a microdomain of active GTPase, as shown for the Rab5/Rabex5/Rabaptin5 proteins functioning on endosomes (Horiuchi *et al.*, 1997; Lippe *et al.*, 2001). The class C/HOPS vacuole tethering complex also contains both a rab GEF and rab effector (Seals *et al.*, 2000; Wurmser *et al.*, 2000). Because Sec2p, Sec4p, and Sec15p are all found on vesicles in transit to sites of secretion, a domain of activated Sec4p on the vesicle surface may be important for polarized vesicle transport and tethering.

The Sec2p localization region negatively regulates the Sec2p–Sec15p interaction. Sec2 proteins missing or mutated in this region bind Sec15p much better than wild type, reflecting increased accessibility of the Sec15p binding site. The growth defects of these *sec2* mutants could be a result of either Sec2p blocking the function of Sec15p or the loss of a free pool of Sec2p. Two arguments support the second possibility: First, these *sec2* alleles are recessive rather than dominant. If they were titrating Sec15p, they would be dominant. Second, although Sec2p truncations cause temperature sensitivity, the expression of just one additional copy of *sec2-59* restores viability at elevated temperatures (Nair *et al.*, 1990; Walch-Solimena *et al.*, 1997). Thus, it is the lack of

sufficient free Sec2p that limits growth of these *sec2* mutants. This is consistent with the observations that nearly all Sec2-78p cosediments with the exocyst (Figure 7) and that over-expression of Sec15p is toxic (Salminen and Novick, 1989). Overexpression of Ypt32p may restore the localization of Sec2-59-GFP and Sec2-78-GFP (Ortiz *et al.*, 2002) by displacing Sec15p from its binding site on the mutant Sec2 proteins, allowing them to recycle onto new vesicles.

Previous fractionation experiments showed that wild-type Sec2p is predominantly cytosolic and that the microsomal pool is bound to vesicles. Truncated Sec2 proteins are enriched in the microsomal pellet, yet flotation gradients showed that the pelletable pool is not membrane bound, but sediments through the formation of a large protein complex (Elkind *et al.*, 2000). Immunoprecipitation experiments with Sec2-59-GFP and Sec2-78-GFP and velocity gradient fractionation confirmed that the pelletable pool of mutant Sec2p is complexed with the exocyst. These results imply that under normal conditions, Sec2p is released from the exocyst complex at some point in the transport reaction. The inability of the *sec2* mutant proteins to dissociate from the exocyst blocks their localization and function. The interaction between the *sec2* mutant proteins and the exocyst could either take place exclusively in the cytosol, where the majority of both reside, or alternatively the complex could initially form on membranes and then persist even after it has been released into the cytosol. Because mutant Sec2 proteins are mislocalized and vesicles are randomly distributed throughout the cytoplasm in *sec2* cells, it is expected that the exocyst would be mislocalized as well. Indeed, the exocyst subunits Sec5-GFPp, Sec8-GFPp, Exo70-GFPp, and Exo84-GFPp, whose localization is known to depend on membrane traffic, are also mislocalized in *sec2-59* cells after a shift to the nonpermissive temperature (Supplemental Figure 4; Zhang *et al.*, 2005).

Insight into the cycle of Sec2p function has come from localization of Sec2-GFP in various *sec* mutants. Sec2-GFP is highly polarized in wild type and in most exocytic mutants (Elkind *et al.*, 2000), reflecting the association of Sec2p with secretory vesicles and the concentration of those vesicles at exocytic sites. The three exceptions in which diffuse fluorescence was seen were the exocyst mutant *sec6-4*, the SNARE mutant *sec9-4*, and the *sec1-1* mutant, defective in SNARE regulation. In these mutants Sec4p still exhibited a strongly polarized localization. These data led to a model in which Sec2p normally recycles after vesicles have become tethered but before membrane fusion. Mutants defective in Sec1p, Sec6p, and Sec9p function are blocked after Sec2p has been released, leading to a polarized accumulation of vesicles carrying Sec4p, but not Sec2-GFP. Other mutants are blocked before this event, leading to an accumulation of vesicles carrying both Sec4p and Sec2-GFP (Elkind *et al.*, 2000). The localization domain of Sec2p may play a key role in this cycle by displacing Sec2p from the exocyst and allowing it to recycle through the cytoplasm so that it can associate with a new round of secretory vesicles. Sec2-GFP localizes properly in *sec15-1* cells (Elkind *et al.*, 2000), consistent with our finding that Sec15-1p binds Sec2p normally (our unpublished data).

A recent study has suggested a role for the elongator complex in Sec2p localization (Rahl *et al.*, 2005). This cytosolic complex is comprised of six subunits, Elp1-6, and is known to covalently modify tRNAs at the wobble position (Huang *et al.*, 2005). Sec2p mislocalizes in *elp1Δ* cells, and ~1% of Sec2p coprecipitates with the elongator complex after cross-linking. The localization domain of Sec2p is necessary, but not sufficient, for the Elp1p interaction. Although the elongator complex does not bind Sec2-59p, *elp1Δ* was identified as a partial suppressor of *sec2-59* (Rahl *et al.*, 2005). Thus, if Sec2-59p mislocalization were the result of a lack of interaction with Elp1p, it is not clear how deletion of *ELP1*
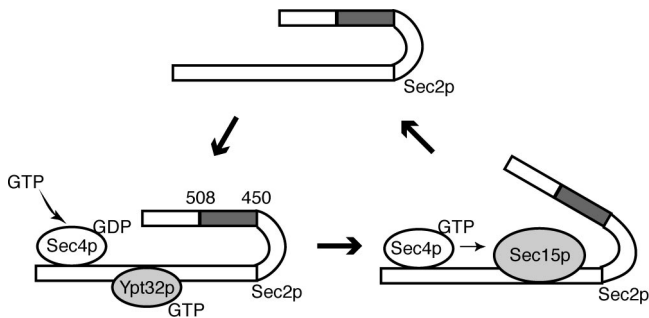
Figure 9. Model of Sec2p function. Sec2p is recruited to secretory vesicles by its interaction with Ypt32p. On the vesicle, Sec2p activates Sec4p. Activated Sec4p in turn recruits its effector Sec15p, which displaces Ypt32p from its binding site on Sec2p. Under normal conditions, Sec2p is released from the exocyst after vesicle tethering. Sec2p mutants defective in the amino acid region 451-508 display increased binding to Sec15p and cannot recycle, which results in mislocalization of Sec2p.

could restore Sec2-59p function. We have found that Sec2-59-GFP remains mislocalized in *elp1*Δ cells (Supplemental Figure 5). To test the possibility that the elongator complex regulates the Sec2p–Sec15p interaction, we have assessed the efficiency of coprecipitation in *elp1*Δ cells. However, no change in the amount of Sec15-13mycp in Sec2-GFP immunoprecipitates was observed upon deletion of *ELP1*. Interestingly, in strains expressing Sec2-59-GFPp or Sec2-78-GFPp, a small increase in the coprecipitation of Sec15p from *elp1*Δ cells was detected (Supplemental Figure 6).

We propose a model (Figure 9), in which Sec2p is recruited to secretory vesicles by its interaction with Ypt32p. Once on the vesicle, Sec2p activates Sec4p, which in turn recruits its effector Sec15p, thereby displacing Ypt32p from its binding site on Sec2p. The association of the Sec4p GEF, Sec2p, with a Sec4p effector, Sec15p, may help to maintain Sec4p in a highly activated state needed for vesicle transport and tethering. Normally, Sec2p is released from the exocyst after tethering to bind a new round of vesicles. Sec2p mutants defective in the region of 450-508 amino acids display increased binding to Sec15p and cannot recycle. This results in mislocalization of Sec2p and defects in secretion. It will be interesting to see whether this mechanism has parallels at other stages of vesicle transport and in higher eukaryotic cells.

ACKNOWLEDGMENTS

REFERENCES

Boyd, C., Hughes, T., Pypaert, M., and Novick, P. (2004). Vesicles carry most exocyst subunits to exocytic sites marked by the remaining two subunits, Sec3p and Exo70p. J. Cell Biol. *167*, 889–901.

Brennwald, P., Kearns, B., Champion, K., Keranen, S., Bankaitis, V., and Novick, P. (1994). Sec9 is a SNAP-25-like component of a yeast SNARE complex that may be the effector of Sec4 function in exocytosis. Cell *79*, 245–258.

Cunningham, K. W., and Wickner, W. T. (1989). Yeast KEX2 protease and mannosyltransferase I are localized to distinct compartments of the secretory pathway. Yeast *5*, 25–33.

Du, L. L., and Novick, P. (2001). Purification and properties of a GTPase-activating protein for yeast Rab GTPases. Methods Enzymol. *329*, 91–99.

Elkind, N. B., Walch-Solimena, C., and Novick, P. J. (2000). The role of the COOH terminus of Sec2p in the transport of post-Golgi vesicles. J. Cell Biol. *149*, 95–110.

Finger, F. P., Hughes, T. E., and Novick, P. (1998). Sec3p is a spatial landmark for polarized secretion in budding yeast. Cell *92*, 559–571.

France, Y. E., Boyd, C., Coleman, J., and Novick, P. J. (2006). The polarity-establishment component Bem1p interacts with the exocyst complex through the Sec15p subunit. J. Cell Sci. *119*, 876–888.

Goud, B., Salminen, A., Walworth, N. C., and Novick, P. J. (1988). A GTP-binding protein required for secretion rapidly associates with secretory vesicles and the plasma membrane in yeast. Cell *53*, 753–768.

Govindan, B., Bowser, R., and Novick, P. (1995). The role of Myo2, a yeast class V myosin, in vesicular transport. J. Cell Biol. *128*, 1055–1068.

Guo, W., Roth, D., Walch-Solimena, C., and Novick, P. (1999). The exocyst is an effector for Sec4p, targeting secretory vesicles to sites of exocytosis. EMBO J. *18*, 1071–1080.

Hattula, K., Furuhjelm, J., Arffman, A., and Peranen, J. (2002). A Rab8-specific GDP/GTP exchange factor is involved in actin remodeling and polarized membrane transport. Mol. Biol. Cell *13*, 3268–3280.

Horiuchi, H., *et al.* (1997). A novel Rab5 GDP/GTP exchange factor complexed to Rabaptin-5 links nucleotide exchange to effector recruitment and function. Cell *90*, 1149–1159.

Huang, B., Johansson, M. J., and Bystrom, A. S. (2005). An early step in wobble uridine tRNA modification requires the Elongator complex. RNA *11*, 424–436.

Karpova, T. S., Reck-Peterson, S. L., Elkind, N. B., Mooseker, M. S., Novick, P. J., and Cooper, J. A. (2000). Role of actin and Myo2p in polarized secretion and growth of *Saccharomyces cerevisiae*. Mol. Biol. Cell *11*, 1727–1737.

Lippe, R., Miaczynska, M., Rybin, V., Runge, A., and Zerial, M. (2001). Functional synergy between Rab5 effector Rabaptin-5 and exchange factor Rabex-5 when physically associated in a complex. Mol. Biol. Cell *12*, 2219–2228.

Nair, J., Muller, H., Peterson, M., and Novick, P. (1990). Sec2 protein contains a coiled-coil domain essential for vesicular transport and a dispensable carboxy terminal domain. J. Cell Biol. *110*, 1897–1909.

Novick, P., and Botstein, D. (1985). Phenotypic analysis of temperature-sensitive yeast actin mutants. Cell *40*, 405–416.

Ortiz, D., Medkova, M., Walch-Solimena, C., and Novick, P. (2002). Ypt32 recruits the Sec4p guanine nucleotide exchange factor, Sec2p, to secretory vesicles; evidence for a Rab cascade in yeast. J. Cell Biol. *157*, 1005–1015.

Pruyne, D. W., Schott, D. H., and Bretscher, A. (1998). Tropomyosin-containing actin cables direct the Myo2p-dependent polarized delivery of secretory vesicles in budding yeast. J. Cell Biol. *143*, 1931–1945.

Puig, O., Caspary, F., Rigaut, G., Rutz, B., Bouveret, E., Bragado-Nilsson, E., Wilm, M., and Seraphin, B. (2001). The tandem affinity purification (TAP) method: a general procedure of protein complex purification. Methods *24*, 218–229.

Rahl, P. B., Chen, C. Z., and Collins, R. N. (2005). Elp1p, the yeast homolog of the FD disease syndrome protein, negatively regulates exocytosis independently of transcriptional elongation. Mol. Cell *17*, 841–853.

Salminen, A., and Novick, P. J. (1989). The Sec15 protein responds to the function of the GTP binding protein, Sec4, to control vesicular traffic in yeast. J. Cell Biol. *109*, 1023–1036.

Seals, D. F., Eitzen, G., Margolis, N., Wickner, W. T., and Price, A. (2000). A Ypt/Rab effector complex containing the Sec1 homolog Vps33p is required for homotypic vacuole fusion. Proc. Natl. Acad. Sci. USA *97*, 9402–9407.

TerBush, D. R., Maurice, T., Roth, D., and Novick, P. (1996). The Exocyst is a multiprotein complex required for exocytosis in *Saccharomyces cerevisiae*. EMBO J. *15*, 6483–6494.

Walch-Solimena, C., Collins, R. N., and Novick, P. J. (1997). Sec2p mediates nucleotide exchange on Sec4p and is involved in polarized delivery of post-Golgi vesicles. J. Cell Biol. *137*, 1495–1509.

Walworth, N. C., and Novick, P. J. (1987). Purification and characterization of constitutive secretory vesicles from yeast. J. Cell Biol. *105*, 163–174.

Wurmser, A. E., Sato, T. K., and Emr, S. D. (2000). New component of the vacuolar class C-Vps complex couples nucleotide exchange on the Ypt7 GTPase to SNARE-dependent docking and fusion. J. Cell Biol. *151*, 551–562.

Zhang, X., Zajac, A., Zhang, J., Wang, P., Li, M., Murray, J., TerBush, D., and Guo, W. (2005). The critical role of Exo84p in the organization and polarized localization of the exocyst complex. J. Biol. Chem. *280*, 20356–20364.